Tetrahedron 64 (2008) 9108–9116

Contents lists available at ScienceDirect

Tetrahedron

journal homepage: www.elsevier.com/locate/tet

Synthesis of π-conjugated, pyridine ring functionalized bis-terpyridines with efficient green, blue, and purple emission

Fu-She Han [a], Masayoshi Higuchi [a,*], Dirk G. Kurth [a,b,*]

[a] Functional Modules Group, Organic Nanomaterials Center, National Institute for Materials Science, 1-1 Namiki, Tsukuba, Ibaraki 305-0044, Japan
[b] Max-Planck-Institute of Colloids and Interfaces, Research Campus Golm, D-14424 Potsdam, Germany

ARTICLE INFO

Article history:
Received 6 June 2008
Received in revised form 30 June 2008
Accepted 30 June 2008
Available online 3 July 2008

Keywords:
Synthesis
Terpyridine
Suzuki coupling
Light-emission
Supramolecule
Polymer
Functional materials

ABSTRACT

A large variety of rigid, π-conjugated, pyridine ring functionalized bis-terpyridines are synthesized efficiently using tandem Miyaura/Suzuki-type cross-coupling reaction. Photophysical property study reveals that the absorption and luminescent properties of the obtained bis-terpyridines are profoundly affected by the nature of the functional groups at the peripheral pyridine and the spacers. Namely, by tailoring precisely the structures, the light-emitting efficiencies of bis-terpyridines can be enhanced significantly with quantum yields (Φ_f) of up to 0.62, and the emission colors can be tuned to display distinct colors including purple, bright blue, and bright green. Consequently, the novel bis-terpyridines are attractive ligands for the assembly of new metallo-supramolecule based functional materials.

1. Introduction

Terpyridines have now evoked widespread interest as functional modules within the domain of supramolecular and coordination chemistry, as well as materials science.[1] This type of compounds has a rich coordination chemistry and generally high binding affinity toward a large variety of transition and rare earth metal cations, giving rise to diverse metallo-supramolecular assemblies with distinct photophysical, photochemical, electrochemical, catalytic, and magnetic properties.[1] In addition, metallo-supramolecular assemblies derived from terpyridines possess a well-defined stereochemistry in contrast to many other modules,[1,2] which is of importance when structure–property relationships are under consideration.

Among the unique properties of terpyridine compounds, their luminescent properties upon coordination with metal ions are particularly attractive due to high potential for technological applications as light-emitting devices and probes in a large spectral range.[1,3] So far, many complexes have been investigated and it has been well demonstrated that the choice of ligand affects profoundly the luminescent properties of the resulting supramolecular assemblies.[1,3] Thus, synthesis of tailored terpyridine modules has become a fundamental step in the construction of high performance metal coordination based functional materials, and indeed, several groups have devoted their efforts to this subject.[4] So far, monotopic terpyridines have been investigated in some detail. As an important contribution, Araki's[4a] and Siegel's[4d] groups have improved significantly the emission properties of monotopic terpyridine compounds by means of structural modification. Polytopic terpyridines have recently attracted considerable interest owing to the advantage of constructing metallo-supramolecular polymers systems.[1e] However, only a few examples have been reported.[4b,5] Furthermore, the available compounds show only a weak efficiency with Φ_f<0.20 in general,[5] and is limited to purple or blue emitting colors with a wavelength maximum at around 400±40 nm.[4,5] Therefore, development of novel polytopic terpyridines with high efficiency as well as other emission colors remains an important challenge.

To this end, we have paid particular attention to rigid, π-conjugated bis-terpyridines because back-to-back ditopic ligands are very useful for the fabrication of structurally well-defined rod-like metallo-supramolecular polymers, avoiding ring formation as detected in flexible[6a] or some rigid angular type analogues.[6b] On the other hand, considering that substituent in the ligand perturbs the photophysical and electronic properties not only of the free ligands[4] but also the final metal complexes,[7] we focused on the investigation into a range of functionalized bis-terpyridines by

* Corresponding authors. Tel.: +81 29 860 4744; fax: +81 29 860 4721.
E-mail addresses: higuchi.masayoshi@nims.go.jp (M. Higuchi), kurth@mpikg.mpg.de (D.G. Kurth).

0040-4020/$ – see front matter © 2008 Elsevier Ltd. All rights reserved.
doi:10.1016/j.tet.2008.06.106

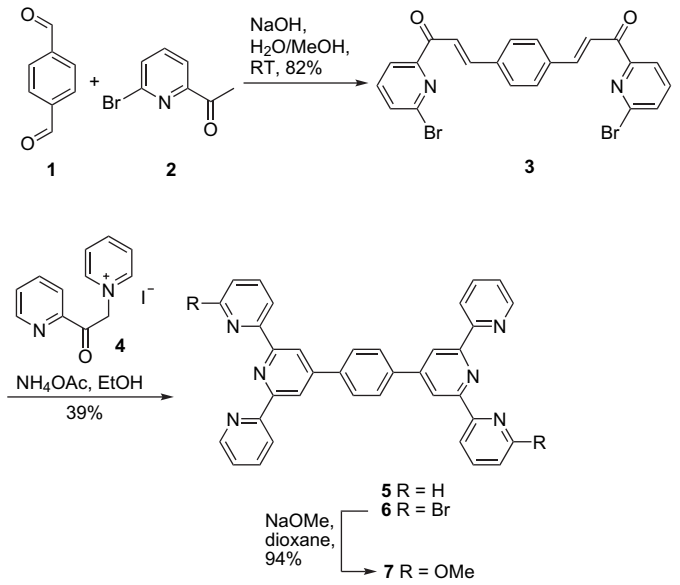

Scheme 1. Synthesis of substituted bis-terpyridines with one phenylene unit as spacer.

appending functional groups at the pyridine periphery and/or by incorporating heteroaromatics into the spacer region. Such compounds are in sharp contrast to the unsubstituted and carbon-aromatic ring bridged bis-terpyridines frequently reported in previous work.[1,8] However, for the synthesis of structurally diverse bis-terpyridines, a general synthetic protocol is highly desired since the conventional approaches such as the Kröhnke method,[9] and substitution or coupling reaction of suitably functionalized mono-terpyridines is often limited in yield and functional group compatibility.[7c,10] Herein, we describe a highly efficient and broadly applicable protocol for the synthesis of various novel bis-terpyridines using palladium-catalyzed tandem Miyaura- and Suzuki-type cross-coupling reactions,[11] which has been shown to be potential for the synthesis of such type of compounds,[12] and the investigation of the photophysical properties of the compounds synthesized.

2. Results and discussion

2.1. Synthesis of various bis-terpyridines

Scheme 1 outlines the Kröhnke approach we utilized here to synthesize compounds **6** and **7**. The reference compound **5** is commercially available from Aldrich. The bromo-substituted compound **6**, which has one phenylene group as spacer, was prepared in two steps involving a Claisen–Schmidt aldol condensation of benzene-1,4-dialdehyde (**1**) and 2-acetyl-6-bromopyridine (**2**), followed by a Michael-type bis-addition of the resulting diazachalcone (**3**) with pyridinium iodide salt (**4**).[9] Nucleophilic substitution reaction of **6** with excess NaOMe gave the dimethoxyl derivative **7**.

For the synthesis of the symmetrically and unsymmetrically substituted derivatives **10**–**15** (Scheme 2), which are bridged by two phenylene units, we have previously developed an efficient protocol by employing Suzuki-type cross-coupling dimerization[11] or a two-step coupling reaction by applying sequentially Miyaura boronic ester formation[13] and Suzuki coupling reaction,[14] since versatile synthesis of these structural variants are troublesome according to the conventional Kröhnke method owing to the limited availability of starting dialdehyde and 2-acetylpyridine derivatives.[15]

On the basis of our previous work, the tandem Miyaura/Suzuki cross-coupling protocol was further employed to synthesize other types of bis-terpyridines, **17**–**24**, featuring the presence of a bent spacer by incorporating various aromatic groups into the spacer region (Scheme 3). While a stepwise procedure is routinely applicable,[11] here, we examined the two-step in situ strategy (Route A and Route B), and found eventually that Route A was even more efficient to access the desired products than the stepwise procedure, although Route B was less effective for heteroaromatic **16** due possibly to the ease of protonolysis of boronic esters formed from *N*- and *S*-heteroaromatic dibromides **16** and diboron **9**.[13a] Thus, mono-terpyridine **8a** (or **8b** and **8c**) was reacted with 1.1 equiv of bis(pinacolato)diboron **9** under Miyaura conditions[13] (5 mol % $PdCl_2(PPh_3)_2$, 3.0 equiv of KOAc, DMF (or DMSO)), until the starting terpyridines **8a**–**c** had disappeared as monitored by TLC.

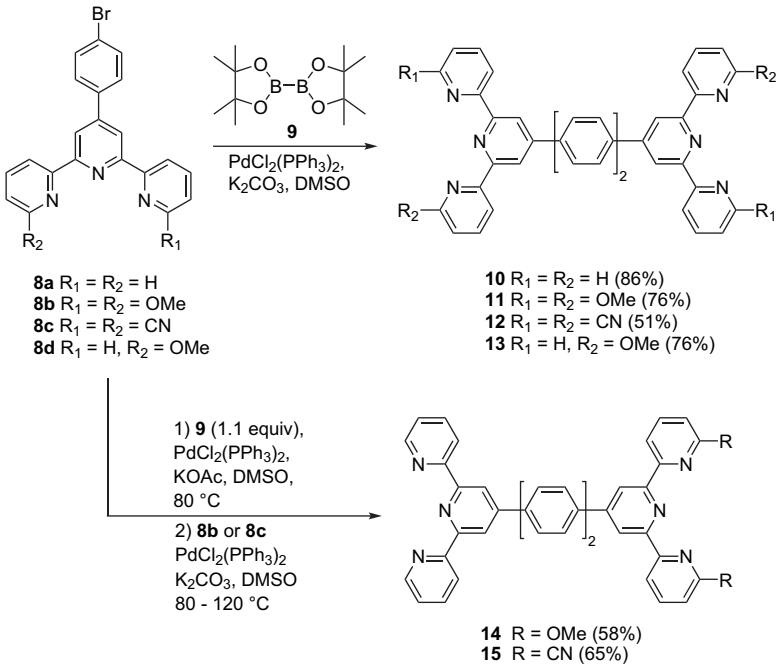

Scheme 2. Synthesis of symmetrically and unsymmetrically substituted ditopic bis-terpyridines with two phenylene units as spacer.[11]

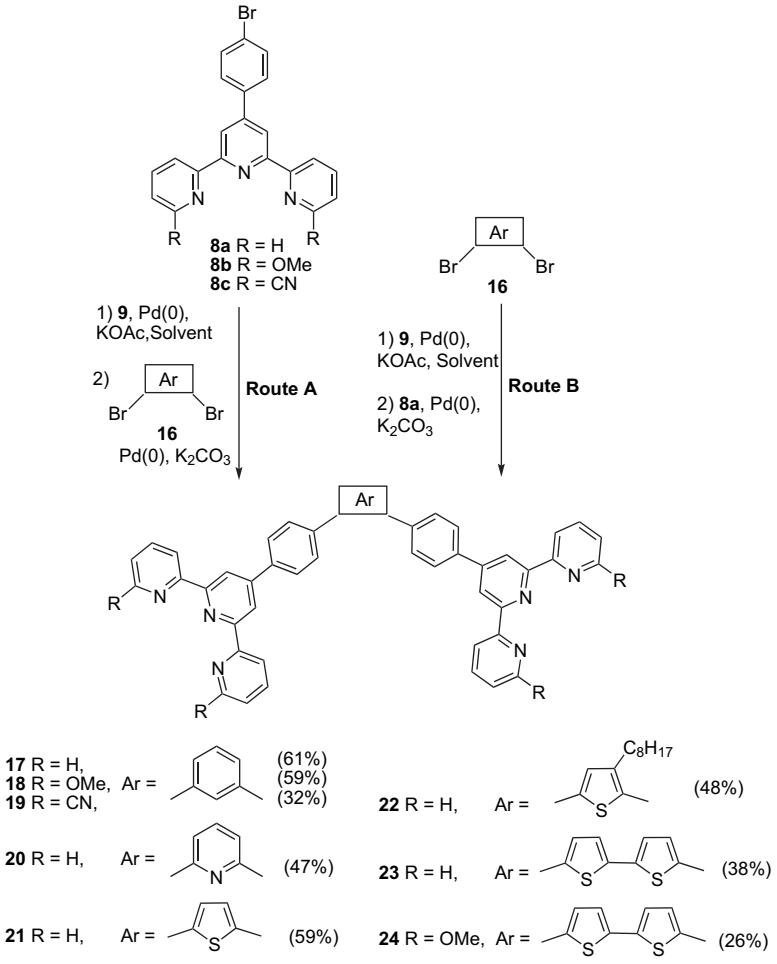

Scheme 3. Synthesis of ditopic bis-terpyridines with diverse spacers.

Then, the reaction vessel was recharged in situ with 0.5 equiv of dibromo compounds **16**, 5 mol % of $PdCl_2(PPh_3)_2$, and 3.0 equiv of K_2CO_3, and the mixture was further heated until the dibromo substrates had disappeared. Purification of the reaction mixture afforded the desired **17**–**24** in moderate to good yields. The structures of these compounds were determined by standard spectroscopic techniques, including ^1H and ^{13}C NMR, and mass analysis.[16] It is now evident that the synthetic protocol presented here is quick and broadly applicable to a large variety of substrates including mono-terpyridine precursors having electron-rich (e.g., **8b**) and deficient groups (e.g., 8**c**), as well as diverse classes of dibromo-aromatic coupling partners such as carbon-aromatic (**10**–**15**, **17**–**19**), *N*- and *S*-heteroaromatic (**20**–**24**), and sterically hindered aromatic compounds (**22**).

It should be noted that, while coupling reaction of **8a**–**c** with 1,4-dibromobenzene was also effective, purification of the resulting products was difficult due to the poor solubility. To compare with the fairly good solubility of bis-terpyridines **17**–**19** derived from the bent 1,3-dibromobenzene, the poor solubility of the analogues prepared from linear-shaped 1,4-dibromobenzene is due probably to the highly symmetric structures.

2.2. Photophysical properties

2.2.1. UV–vis absorption property

With a diverse class of novel bis-terpyridines in hand, we next investigated their photophysical properties. For the absorption behavior, a general observation is that, when compared to reference compound **5**, the maximum absorption band (λ_{abs}) of the bis-terpyridines having carbon-aromatic (**6**, **7**, **10**–**15**, and **17**–**19**) and *N*-heteroaromatic spacers (**20**) is around 300 nm, which is red-shifted slightly (ca. 10±4 nm) by appending either the electron-donating OMe or electron-withdrawing Br and CN substituents at the peripheral pyridines (Table 1). In sharp contrast, the λ_{abs} red shifts significantly to ca. 370 nm by introducing a thiophene group in the spacer region (**21**), and moves further to more than 400 nm when a bi-thiophene group (**23** and **24**) is incorporated (Table 1 and Fig. 1). It should be noted that, while interposing a thiophene ring without substituent at 3- or 4-position in the spacer region leads to a large red-shift of λ_{max}, attaching an octyl alkyl chain at the 3-position of thiophene unit moves the absorption maximum from 370 to 321 nm as a comparison of **21** and **22** shows, indicating substitution at the 3- or 4-position of thiophene ring affects markedly on the absorption behavior of bis-terpyridine derivatives. This observation is attributed obviously to the introduction of a long alkyl chain, which causes a twist between the thiophene and phenylene rings, and ultimately, resulting in a decreased π-conjugation between the aromatic rings.[7c,17] It should also be mentioned that, extending the length of spacer generally shifts the λ_{abs} toward longer wavelength, the λ_{abs} of compounds **17**–**19**, whose two terpyridine moieties are bridged by three contiguous but angularly connected phenylene rings, are slightly shifted toward shorter wavelength to compare with compounds **10**, **11**, and **15**, whose two terpyridine moieties are bridged by two linearly linked phenylene

Table 1
Absorption and emission properties of various bis-terpyridines

	λ_{abs} (nm)[a] (log ε)	λ_{em}[b]	Φ_f[c]
5	292 (4.79)	360	0.13
6	297 (4.85)	357	0.08
7	298 (4.84)	373	0.22
10	310 (4.78)	371	0.37[d]
11	313 (4.95)	376	0.54
13	313 (4.92)	371	0.62
14	314 (4.92)	371	0.59
15	298 (4.78)	384	0.41
17	288 (4.84)	364	0.23
18	310 (5.01)	371	0.36
19	295 (4.82)	381	0.21
20	290 (4.86)	364	0.58
21	370, 280 (4.66,4.41)	445, 457	0.44
22	321, 280 (4.65,4.64)	441, 384	0.42
23	403, 280 (4.61,4.63)	500, 472	0.20
24	410, 305 (4.69,4.67)	505, 474	0.31

[a] In 1×10^{-5} M CH_2Cl_2 solution.
[b] In 5×10^{-7} M CH_2Cl_2 solution with absorbance <0.1. The excitation wavelength was 290 nm for compounds **17** and **20**; 300 nm for **5**–**7** and **10**–**15**; 310 nm for **11**; 320 nm for **22**; 370 nm for **21**; 400 nm for **23**; and 410 nm for **24**.
[c] Determined relative to bis-terpyridine **5**, Φ_f=0.13.
[d] Φ_f=0.49 in reported literature (see Ref. 5a).

units. The absorption spectral change is presumably due to the fact that an angular connection may introduce an additional steric interaction between the two terpyridine fragments, which prohibits an effective planar conjugation of the aromatic rings as compared to the linearly connected analogues.[4d]

The molar absorptivity (log ε in Table 1) also correlates with the substituents and spacers. As listed in Table 1, we observe clearly that introduction of either electron-donating (OMe) or electron-withdrawing group (Br and CN) increases the molar absorptivity as compared to **5**. As for the effect of spacer, compounds with carbon-aromatic and *N*-heteroaromatics in the spacer region show an enhanced molar absorptivity, which is decreased, however, after replaced by *S*-heteroaromatics **21**–**24**.

2.2.2. Emission property

The light-emitting property of various bis-terpyridines is also investigated. As can be seen from Table 1, photoluminescence of the obtained bis-terpyridines is affected prominently by the nature of spacers and substituents. Thus, the maximum emission band (λ_{em}) of the carbon-aromatic (**6**, **7**, **10**–**15**, and **17**–**19**) and *N*-heteroaromatic ring (**20**) bridged compounds is located at about 370 nm, displaying a purple color (Table 1, and Fig. 2). Compounds **21** and **22**, which contain one thiophene ring in the spacer region, exhibit bright blue emission color with λ_{em} at ca. 450 nm for **21**. More excitingly, by further increasing the number of thiophene from one to two units, the emitting wavelength of **23** and **24** is red-shifted to more than 500 nm paired with a shoulder at ca. 470 nm, showing that a large Stokes' shift occurred (>90 nm). Consequently, the emission colors of **23** and **24** are bright green. The green emission of polytopic terpyridines has not been reported in the literature so far. Thus, our results show that the emission color of this class of compound can be tuned from purple via blue to green by structural modification. On the basis of these results, we believe that the emission color can be further extended to red by tuning the structure of the ligands.

To elucidate the effect of spacers on the photophysical properties, the electronic states of compounds **10**, **17**, and **21**, which represent the types of spacers with different nature such as linear **10** vs angular **17**, and carbon-aromatic **17** vis heteroaromatic **21**, were calculated using MOPAC/AM1 and PM5, respectively. The HOMO and LUMO molecular orbitals for **10** were deduced from its X-ray structure,[7a,11] while those for compounds **17** and **21** were calculated by fixing the dihedral angle between the terpyridine unit and the

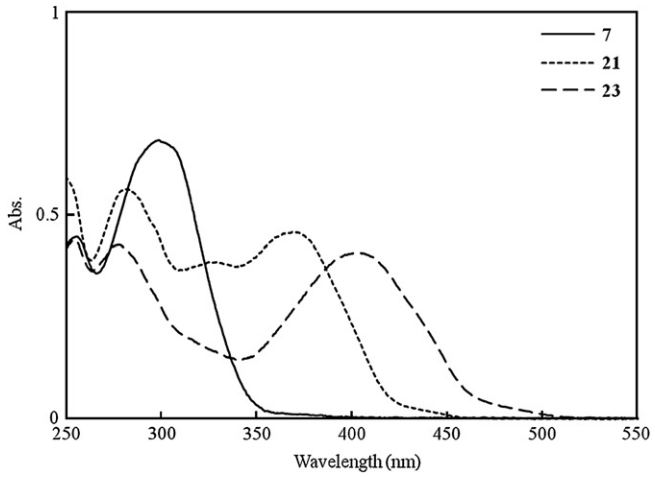

Figure 1. UV–vis spectra of selected bis-terpyridines **7**, **21**, and **23** in CH_2Cl_2 (1×10^{-5} M).

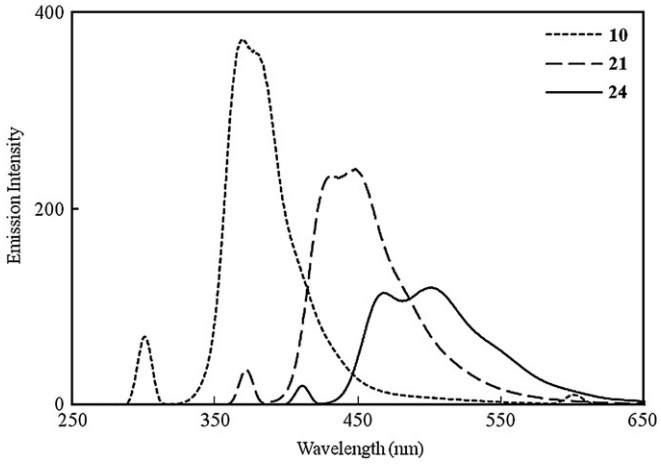

Figure 2. Emission colors of selected compounds **10**, **21** and **24** (from left to right) in CH_2Cl_2 excited with a 365 nm UV lamp (top) and their corresponding emission spectra in 5×10^{-7} M CH_2Cl_2 solution (bottom). The small peaks in the emission spectra are due to an optical artifact (excitation wavelength: 310, 370, and 410 nm for compounds **10**, **21**, and **24**, respectively).

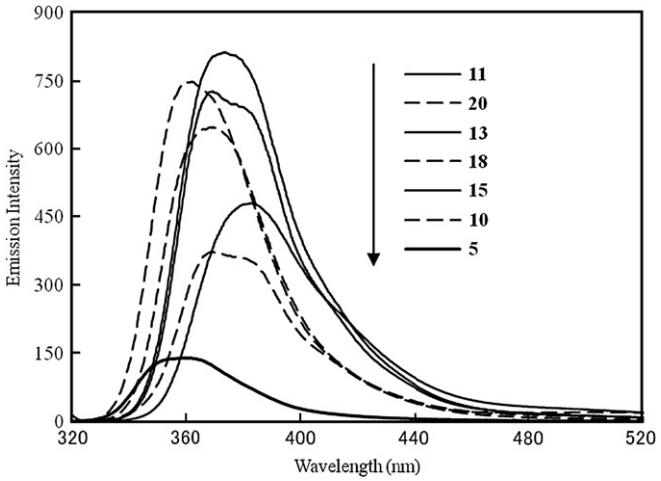

Figure 3. Effect of bis-terpyridine structures on the emission intensity referenced to **5**. The spectra are measured in 5×10^{-7} M CH_2Cl_2 solution.

collected phenylene ring to 27.976° based on the X-ray structure of **10**.

The results showed that using either AM1 or PM5 method, the HOMO and LUMO of the linear-shaped **10** are located on the phenylene ring as denoted with π_{ph} and π^*_{ph}, respectively. Thus, the lowest energy absorption for **10** is due to the π_{ph}–π^*_{ph} transition. For angular **17**, the HOMO orbital is mainly located on the central phenylene ring (π_{c-ph}), while the LUMO appears mainly on the phenylene ring linked to the terpyridine unit (π^*_{ph-tpy}), and consequently, the lowest energy band for **17** is attributed mostly to intramolecular charge transfer (ICT) of π_{c-ph} to π^*_{ph-tpy}. The different energy transition states between **10** and **17** are consistent with their optimized conformers, where the dihedral angle between the two directly linked phenylene rings in **10**[7a] and **17** are 27.302° and ca. 46.282°, respectively. Thus, the larger dihedral angle exhibited in **17** results in a smaller π-conjugation when compared to **10**, giving rise to an increased energy gap between the LUMO and HOMO for **17** (8.170 eV) as compared to that of **10** (7.841 eV). These calculated results are in good agreement with the observed absorption property with **17** showing a λ_{max} of ca. 22 nm shorter than **10** (Table 1).

Somewhat different from **10** and **17**, compound **21** containing a thiophene ring in the spacer region leads to a conjugation between the thiophene and phenylene rings. Both the HOMO and LUMO orbitals are located on the conjugated region consisting of phenylene/thiophene/phenylene rings with the major part on thiophene ring, as represented by π_{ptp} and π^*_{ptp}, respectively. Thus, the lowest energy absorption in the case of **21** is a local transition of π_{ptp} to π^*_{ptp}. Due to the large conjugation, the energy gap between the LUMO and HOMO is significantly decreased to 7.360 eV, and ultimately, leading to a red-shifted emission and absorption for the thiophene-bridged compounds as seen from their photophysical properties.

As for the emission efficiency, we observed that in general, attachment of electron-donating OMe group to the pyridine ring or extending appropriately the conjugation length of the spacers give rise to an increased quantum yield (Φ_f).[18] Accordingly, among the 16 representatives, compounds **11**, **13**, and **14** (Table 1), which have an extended spacer as well as electron-donating OMe groups at pyridine periphery, and **20**, which contains a pyridine ring, exhibit a significantly increased Φ_f of larger than 0.54, with a maximum Φ_f of up to 0.62 for **13**, in contrast to Φ_f=0.13 of reference compound **5**. Compounds, which are modified either by extending the spacer only or by appending electron-donating group only (**10**, **15**, **18**, **21**, and **22**), also show high efficiencies ranging from 0.36 to 0.44. In addition, the fluorescence intensity of these compounds is increased by 4–6 times as compared to compound **5** (Fig. 3). However, electron-withdrawing groups, such as Br and CN, generally lead to a decreased emission efficiency when **6** and **7**, **14** and **15**, and **18** and **19** are parallelly compared. It should be noted that, while Φ_f increases when the length of the spacer is extended, incorporation of a second thiophene ring causes a decrease in Φ_f as a comparison of **21** and **23** shows. However, on the basis of the principal rules observed, the quantum yield of the green emitters was increased effectively from 0.20 for **23** to 0.31 for **24** by introducing OMe functionalities.

2.2.3. Solvent effect on the photophysical properties

To examine the solvent effect on the photophysical property, several selected compounds were investigated in various solvent systems. The results show that the photophysical behavior of the angular bis-terpyridine derivatives such as **17**, **18**, and **20** are similar to the linear-shaped compounds such as **6**, **10**, and **13** in different solvent systems, indicating that the photophysical properties are less dependent on the shape of spacers. Thus, for a clear discussion of the effect of substituents and the length of spacers on the photophysical properties, the UV–vis and fluorescence data of five representatives **6**, **10**, **13**, **21**, and **23** are compared in more detail. As can be seen from the data collected in Table 2, the absorption maximum for each compound is essentially identical in aprotic polar CH_3CN and CH_2Cl_2, and in protic MeOH. However, use of nonpolar cyclohexane shifts the band toward shorter wavelength of about 10 nm. Only a negligible difference is observed for the absorption intensity (data not shown) by varying the solvents except that **13** and **23** show a relatively large decrease in ε_{max} associated with a broadened band shape in MeOH solution. This is due probably to the poor solubility of **13** and **23** in MeOH as seen from the somewhat opaque solution. Also, the emission efficiencies (data not shown) are less influenced by changing the solvent except for **13** and **23** whose emission intensity decrease to about half in MeOH compared to that in other solvents mainly due to the solubility problem, although hydrogen bonding is possibly an additional factor as being observed in some individuals of monoterpyridines.[4c]

Table 2
Effect of solvent polarity on the photophysical properties of various bis-terpyridines[a]

Solvent	**6**		**10**		**13**		**21**		**23**	
	λ_{abs} (nm)	λ_{em} (nm)	λ_{abs} (nm)	λ_{em} (nm)	λ_{abs} (nm)	λ_{em} (nm)	λ_{abs} (nm)	λ_{em} (nm)	λ_{abs} (nm)	λ_{em} (nm)
C_6H_{12}[b]	288	348, 357	298	361, 375	308	361, 375	362, 279	439, 417	394, 275	486, 459
CH_2Cl_2	297	357	310, 299	371	313	371	370, 280	445, 427	403, 281	500, 472
CH_3CN[b]	295	359	308, 297	375	311	374	368, 279	447	400, 275	486[c]
MeOH[b]	297	360	311, 299	380	314	381	370, 280	452	403, 280	490[c]

[a] Measured in 1×10^{-5} M for UV–vis absorption (λ_{abs}) and 5×10^{-7} M for emission (λ_{em}), respectively. The excitation wavelength was 300 nm for **6**, **10**, and **13**, 370 nm for **21**, and 400 nm for **23**.
[b] Containing 10% CH_2Cl_2 due to the poor solubility of the compounds in pure MeOH, CH_3CN, and cyclohexane (C_6H_{12}).
[c] Middle position of a broad band.

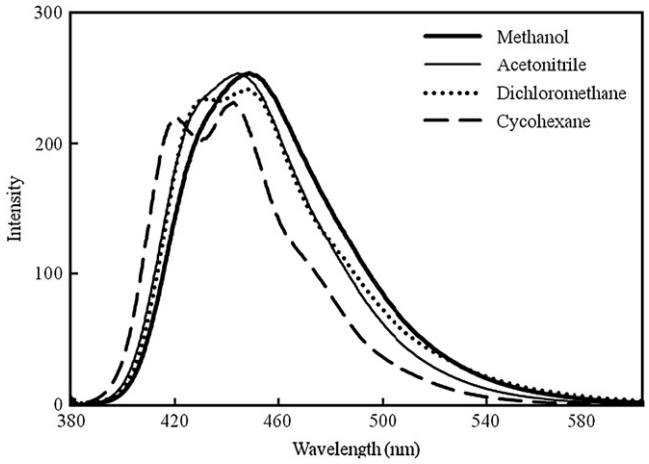

Figure 4. Emission spectra of bis-terpyridine **21** excited at 370 nm in 5×10^{-7} M solution in various solvents.

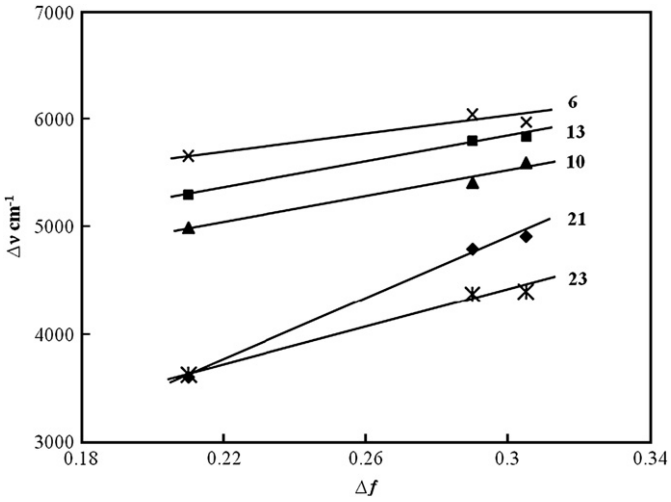

Figure 5. Lippert–Mataga plot for **6**, **10**, **13**, **21**, and **23** in different solvents. The difference between the maximal wavenumbers of absorption and fluorescence spectra ($\Delta\nu$) is plotted as a function of solvent polarity according to Lippert's function (Δf).[4e,19]

In contrast, the emission wavelength for each compound depends on the solvent. Upon increasing the solvent polarity[19] from cyclohexane via CH_2Cl_2 and CH_3CN to MeOH without considering the protic nature of MeOH,[4c] the emission maximum shifts gradually toward longer wavelength as seen from the data in Table 2 and the emission spectra of a representative example **21** depicted in Figure 4. This bathochromic shift is more pronounced when the length of spacer for bridging the two terpyridine moieties increases, showing an enlarged $\Delta\nu$ ($\nu_{Hex}-\nu_{MeOH}$) of ca. 958, 1358, 1454, and 1857 cm^{-1} for compounds **6**, **10**, **13**, and **21**, respectively. On the other hand, the bathochromic effect of substitution in pyridine periphery on the emission property is rather weak when unsubstituted **10** and OMe modified ligands **13** are compared. These results indicate that the excited states of bis-terpyridine compounds are stabilized as a consequence of increasing solvent polarity, and the magnitude of stabilization is correlated mainly with the length of spacer.

Equally interesting to the spectral shift, another noticeable feature of the fluorescence spectra is the strong solvent dependence of the emission band shape. As a representative example, compound **21** shows an unstructured, relatively broad emission profile in polar solvent such as MeOH and CH_3CN as can be seen in Figure 4. By decreasing the solvent polarity, e.g., from CH_3CN via CH_2Cl_2 to cyclohexane, the observed band shape becomes gradually more structured, giving rise to two distinctly resolved bands in non-polar cyclohexane. Such a behavior combined with solvent-dependent response of the spectral shift (vide supra) is well known in electron donor–acceptor dyads[20] and has also been noted for a bis-terpyridine compound,[7c] and is attributed to close π–π^* interactions and the formation of a fluorescent intramolecular charge transfer (ICT) sate in polar solvent, which is destabilized in non-polar solvent.[21]

$$\Delta\nu = \Delta\nu_{abs} - \Delta\nu_{em} = \frac{2(\Delta\mu)^2}{hca^3}\Delta f + \text{Const.} \quad (1)$$

$$\Delta f = \left[\frac{\varepsilon-1}{2\varepsilon+1} - \frac{n^2-1}{2n^2+1}\right] \quad (2)$$

To estimate the dipole moment difference ($\Delta\mu$) between the ground and excited state of the functionalized bis-terpyridines, plots of the difference between the maximal wavenumber (1/wavelength) of the absorption and fluorescence spectra ($\Delta\nu$) as a function of solvent polarity (Δf) are made according to the Lippert–Mataga function as shown in Eqs. 1 and 2,[4e,19] where Δf is the Lippert's solvent polarity parameter, ε and n are the dielectric constant and the refractive index of the medium, respectively, a is the effective radius of the Onsager cavity of a compound, h and c correspond to Planck's constant and the velocity of light, respectively.

No good correlation is found for most cases with the $\Delta\nu$ values in cyclohexane exhibiting a large deviation from the curve fitting. However, plots of the spectral shifts in CH_2Cl_2, CH_3CN, and MeOH show a satisfactory linear correlation with solvent polarity as depicted in Figure 5. Generally, the spectral shifts of **6**, **10**, and **13**, which have one or two phenylene units in the spacer region as well as different substituents in the pyridine rings such as electron-deficient Br (**6**), neutral H (**10**), and electron-rich OMe groups (**13**), are moderately sensitive to the solvent polarity. In contrast, compounds **21** and **23** having thiophene spacers exhibit a considerable spectral shift upon increasing the solvent polarity. Assuming a value of 9–11 Å (ca. 5 Å for half molecule[4e]) for the effective radius of the Onsager cavity, $\Delta\mu$ for **6**, **10**, **13**, **21**, and **23** deduced from the Lippert–Mataga equation is about 2.0±0.3, 2.1±0.3 (for compounds **10** and **13**), 3.8±0.5, and 3.2±0.4 D, respectively. These results further indicate that the magnitude of the bathochromic shift correlates mainly with the type of spacers, while effect of the substituents is weak.

3. Conclusion

In summary, novel rigid, π-conjugated bis-terpyridines having various substituents and aromatic spacers were synthesized using a one-pot Suzuki-type cross-coupling strategy. The synthetic protocol is simple, quick, and applicable to access a large number of new bis-terpyridine derivatives. The photophysical properties of the obtained compounds are presented. On the basis of our results, we can make several principal conclusions: (i) the maximum absorption (λ_{abs}) is affected significantly by the types of spacers, and ultimately, λ_{abs} can be tuned to cover a range from ca. 300 nm to more than 400 nm; (ii) molar absorptivity is mainly influenced by the electronic properties of the substituents at the pyridine periphery, although an additional contribution of the spacer is observed. Thus, appending an electron-donating OMe group results in a markedly enhanced extinction coefficient exceeding 10^5 M^{-1} cm^{-1}; (iii) the affecting tendency of substituents and spacers on photoluminescent property is in consistent with the absorption behavior. Thus, λ_{em} can be tuned to span the region from ca. 370 nm to more than 500 nm by changing the spacer, and the

emission efficiency (Φ_f) is significantly increased to 0.62 by appending OMe group. Consequently, the newly synthesized bis-terpyridines exhibit three distinct emission colors, namely, purple, bright blue, and bright green. In addition, we have shown that the fluorescence spectra of the bis-terpyridines are dependent on the solvent polarity. Thus, these novel compounds are promising candidates for the construction of metallo-supramolecular based light-emitting polymers. Further work concerning the photophysical properties of the polymer materials is currently underway in our laboratory.

4. Experimental section

4.1. General methods

Unless otherwise noted, all reagents were of reagent grade and were used without purification. Reaction solvents were dehydrated and were purchased from Wako or Kanto Chemical Co., Inc. Deionized H_2O was used in the experiment where required. ^1H NMR and ^{13}C NMR spectra were recorded at 300 and 75 MHz, respectively, on a JEOL AL 300/BZ instrument. Chemical shifts were given relative to TMS. Mass spectra (MS) were measured by using AXIMA-CFR, Shimadzu/Kratos TOF Mass spectrometer. High resolution mass spectra (HRMS) were measured by using Shimadzu LCMS-IT-TOF spectrometer. UV–vis spectra were recorded using a Shimadzu UV-2550 UV–vis spectrophotometer. Emission spectra were measured using Shimadzu RF-5300PC spectrofluorophotometer. MeOH, CH_3CN, CH_2Cl_2, and cyclohexane for photophysical measurement are special solvents for luminescent analysis and were purchased from Kanto Chemical Co., Inc. Analytical thin layer chromatography (TLC) was performed using Merck aluminum oxide 60 F_{254} neutral or silica gel 60 F_{254} coated on aluminum sheets (20×20 cm). Flash column chromatographic separations were performed on silica gel 60N (neutral, 40–100 μM), Kanto Chemical Co. Inc., or activated alumina oxide (75 μM), Wako.

4.1.1. Synthesis of dibromo-bis-terpyridine (*6*)

To a 200 mL MeOH solution of benzene-1,4-dicarboxaldehyde **1** (3.62 g, 26.99 mmol) was added 2-acetyl-6-bromopyridine **2** (10.80 g, 53.98 mmol) and 10% aqueous NaOH (2.16 g in 20 mL H_2O) at room temperature, and the mixture was stirred at room temperature overnight. The precipitate formed was collected by filtration, and washed sequentially with H_2O and MeOH for three times, respectively. The slight yellow solid was then dried in vacuo to give diazachalcone **3** (10.5 g, 78%), which was used directly for the following reaction without further purification. To a 200 mL EtOH solution of crude **3** (7.1 g, 14.26 mmol) was added pyridinium iodide salt **4** (9.3 g, 28.53 mmol) and NH_4OAc (54.0 g, 0.70 mol). The solution was refluxed for 60 h and then cooled to room temperature. The precipitate formed upon cooling was collected by filtration, and washed sequentially with H_2O and MeOH for three times, respectively. The crude product was purified by column chromatography on basic Al_2O_3 (CH_2Cl_2/hexane 5:1 then pure CH_2Cl_2) to give **6** (3.88 g, 39%) as white powder; mp>300 °C; ^1H NMR ($CDCl_3$) δ=8.82 (d, 2H, J=1.9 Hz), 8.77 (d, 4H, J=1.8 Hz), 8.66 (dd, 4H, J_1=7.7 Hz, J_2=0.9 Hz), 8.06 (s, 4H), 7.90 (dt, 2H, J_1=7.7 Hz, J_2=1.8 Hz), 7.45 (t, 2H, J=7.7 Hz), 7.55 (dd, 2H, J_1=7.7 Hz, J_2=0.9 Hz), 7.38 (ddd, 2H, J_1=7.7 Hz, J_2=4.8 Hz, J_3=0.9 Hz); ^{13}C NMR ($CDCl_3$) δ=157.6, 156.3, 156.1, 154.6, 149.9, 149.3, 141.7, 139.2, 139.1, 136.8, 128.1, 128.0, 123.9, 121.4, 120.1, 119.5, 119.3; MALDI-MS: m/z (%)=699 (100) $[M+H]^+$; HRMS found m/z: 699.0347 $[M+H]^+$; $C_{36}H_{23}Br_2N_6$ requires: 699.0330.

4.1.2. Synthesis of dimethoxyl bis-terpyridine (*7*)

To a 60 mL dioxane solution of **6** (200 mg, 0.287 mmol) was added NaOMe (1.0 M solution in MeOH, 1.72 mmol). The solution was refluxed for 2 days under N_2 atmosphere. Solvent was evaporated under reduced pressure and the residue was suspended in 200 mL $CHCl_3$. The suspension was then washed with H_2O (50 mL) for three times. The organic layer was separated, dried over $MgSO_4$, filtered, concentrated, and purified by column chromatography on activated basic Al_2O_3 (hexane/CH_2Cl_2=9:1 then pure CH_2Cl_2) to give **7** (161 mg, 96%) as white powder; mp>300 °C; ^1H NMR ($CDCl_3$) δ=8.78 (s, 2H), 8.77 (s, 2H), 8.75 (d, 2H, J=8.1 Hz), 8.69 (d, 2H, J=8.0 Hz), 8.30 (d, 2H, J=7.5 Hz), 8.04 (s, 4H), 7.87 (br t, 2H, J=7.5 Hz), 7.78 (t, J=7.5 Hz), 7.36 (dd, 2H, J_1=7.5 Hz, J_2=4.8 Hz), 6.84 (d, 2H, J=8.1 Hz), 4.13 (s, 6H); MALDI-MS: m/z (%)=601 (100) $[M+H]^+$; HRMS found m/z: 601.2359 $[M+H]^+$; $C_{38}H_{29}N_6O_2$ requires: 601.2352.

4.2. General procedure for the synthesis of symmetric bis-terpyridines via Suzuki-type dimerization (10–13)

To a 30 mL DMSO solution of mono-terpyridine (**8a–d**, 0.773 mmol) was added bis(pinacolato)diboron **9** (102 mg, 0.402 mmol), K_2CO_3 (320 mg, 2.318 mmol), and $PdCl_2(PPh_3)_2$ (27 mg, 0.039 mmol). The solution was stirred at 80–120 °C under an argon atmosphere until the starting material had disappeared as monitored by TLC. The catalyst was removed by filtration and washed with $CHCl_3$ after the reaction mixture was cooled to room temperature. The filtrate was then washed with H_2O (50 mL) for five times, and the organic layer was dried over $MgSO_4$, filtered, concentrated, and purified by column chromatography on activated basic Al_2O_3 (hexane/CH_2Cl_2 4:1 then pure CH_2Cl_2) to give the dimerized products **10–13**.

4.2.1. Symmetric bis-terpyridine *10*

White powder, 86% yield from **8a**; ^1H NMR ($CDCl_3$) δ=8.82 (s, 4H), 8.75 (ddd, 4H, J_1=5.4 Hz, J_2=1.8 Hz, J_3=0.9 Hz), 8.69 (d, 4H, J=7.8 Hz), 8.04 (d, 4H, J=8.1 Hz), 7.89 (td, 4H, J_1=8.1 Hz, J_2=1.8 Hz), 7.83 (d, 4H, J=8.4 Hz), 7.37 (dd, 4H, J_1=7.8 Hz, J_2=4.8 Hz); ^{13}C NMR ($CDCl_3$) δ=156.3, 156.1, 149.7, 149.2, 141.1, 137.7, 136.9, 127.8, 127.6, 123.8, 121.4, 118.8; MALDI-MS: m/z (%)=617 (100) $[M+H]^+$; HRMS found m/z: 617.2470 $[M+H]^+$; $C_{42}H_{29}N_6$ requires: 617.2454.

4.2.2. Symmetric bis-terpyridine *11*

White powder, 76% yield from **8b**; ^1H NMR ($CDCl_3$) δ=8.72 (s, 4H), 8.30 (d, 4H, J=7.2 Hz), 7.98 (d, 4H, J=8.4 Hz), 7.87 (d, 4H, J=8.4 Hz), 7.78 (t, 4H, J=7.8 Hz), 6.83 (d, 4H, J=8.1 Hz), 4.12 (s, 12H); ^{13}C NMR ($CDCl_3$) δ=163.8, 156.1, 153.9, 139.4, 130.8, 128.8, 127.8, 127.7, 127.4, 118.6, 114.2, 111.1, 53.3; MALDI-MS (%): m/z=737 (100) $[M+H]^+$; HRMS found m/z: 737.2875 $[M+H]^+$; $C_{46}H_{37}N_6O_4$ requires: 737.2876.

4.2.3. Symmetric bis-terpyridine *13*

White powder, 76% yield from **8d**; ^1H NMR ($CDCl_3$) δ=8.78 (d, 2H, J=1.8 Hz), 8.76 (d, 2H, J=1.8 Hz), 8.75 (ddd, 2H, J_1=4.2 Hz, J_2=1.8 Hz, J_3=0.9 Hz), 8.70 (dt, 2H, J_1=7.8 Hz, J_2=1.2 Hz), 8.30 (dd, 2H, J_1=7.2 Hz, J_2=0.8 Hz), 8.02–8.00 (m, 4H), 7.91 (dd, 2H, J_1=7.5 Hz, J_2=1.8 Hz), 7.87–7.84 (m, 4H), 7.78 (dd, 2H, J_1=8.1 Hz, J_2=7.2 Hz), 7.37 (ddd, 2H, J_1=7.5 Hz, J_2=4.8 Hz, J_3=1.2 Hz), 6.84 (dd, 2H, J_1=8.1 Hz, J_2=0.8 Hz); ^{13}C NMR ($CDCl_3$) δ=163.7, 156.4, 156.1, 156.0, 153.7, 149.6, 149.1, 141.1, 139.4, 138.2, 136.9, 127.8, 127.7, 123.8, 121.4, 118.7 (2C), 114.1, 111.2, 53.3; MALDI-MS: m/z (%)=677 (100) $[M+H]^+$; HRMS found m/z: 677.2652 $[M+H]^+$; $C_{44}H_{33}N_6O_2$ requires: 677.2665.

4.3. General procedure for the synthesis of unsymmetric bis-terpyridines via tandem Miyaura/Suzuki coupling (14 and 15)

To a 8 mL DMSO solution of **8a** (100 mg, 0.258 mmol) was added bis(pinacolato)diboron **9** (72 mg, 0.283 mmol), KOAc (76 mg,

0.773 mmol), and $PdCl_2(PPh_3)_2$ (9.0 mg, 0.013 mmol). The solution was stirred at 80 °C under argon atmosphere for 12 h. The reaction vessel was recharged with K_2CO_3 (107 mg, 0.773 mmol), **8b** (or **8c**) (0.258 mmol), and Pd catalyst (5 mol %) after being diluted with additional 8 mL DMSO. The mixture was then heated at 80–120 °C until **8b** (or **8c**) had disappeared as monitored by TLC. The catalyst was removed by filtration and washed with $CHCl_3$ after the reaction mixture was cooled to room temperature. The filtrate was then washed with H_2O (50 mL) for five times, and the organic layer was dried over $MgSO_4$, filtered, concentrated, and purified by column chromatography on activated basic Al_2O_3 to give **14** and **15**, respectively.

*4.3.1. Unsymmetric bis-terpyridine **14***

White powder, 58% yield from **8a** and **8b**; ^{1}H NMR ($CDCl_3$) δ=8.82 (s, 2H), 8.75 (ddd, 2H, J_1=5.7 Hz, J_2=1.8 Hz, J_3=0.9 Hz), 8.72 (s, 2H), 8.70 (d, 2H, J=7.8 Hz), 8.29 (dd, 2H, J_1=7.5 Hz, J_2=0.9 Hz), 8.05 (d, 2H, J=7.5 Hz), 7.97 (d, 2H, J=7.2 Hz), 7.90 (ddd, 2H, J_1=J_2=7.8 Hz, J_3=1.8 Hz), 7.87 (d, 2H, J=8.7 Hz), 7.81 (d, 2H, J=6.9 Hz), 7.76 (d, 2H, J=7.8 Hz), 7.37 (dd, 2H, J_1=J_2=6.6 Hz), 6.83 (d, 2H, J=7.8 Hz), 4.12 (s, 6H); ^{13}C NMR ($CDCl_3$) δ=163.6, 156.3, 156.0, 155.9, 153.7, 149.7, 149.4, 149.2 (2C), 141.0, 139.4, 138.4, 137.7, 136.9, 127.9, 127.7 (2C), 127.6, 123.9, 121.4, 118.7, 118.6, 114.1, 111.1, 53.3; MALDI-MS (%): m/z=677 (100) $[M+H]^+$; HRMS found m/z: 677.2652 $[M+H]^+$; $C_{44}H_{33}N_6O_2$ requires: 677.2665.

*4.3.2. Unsymmetric bis-terpyridine **15***

White powder, 65% yield from **8a** and **8c**; ^{1}H NMR ($CDCl_3$) δ=8.90 (s, 2H), 8.88 (dd, 2H, J_1=8.1 Hz, J_2=1.2 Hz), 8.83 (s, 2H), 8.76 (dd, 2H, J_1=3.6 Hz, J_2=0.9 Hz), 8.70 (d, 2H, J=8.1 Hz), 8.08–8.01 (m, 6H), 7.92–7.87 (m, 4H), 7.85 (d, 2H, J=8.1 Hz), 7.78 (dd, 2H, J_1=7.8 Hz, J_2=1.2 Hz), 7.37 (ddd, 2H, J_1=J_2=7.5 Hz, J_3=1.8 Hz); ^{13}C NMR ($CDCl_3$) δ=157.6, 156.5, 156.2, 154.3, 149.2, 141.9, 140.9, 137.9, 136.8 (2C), 133.6, 132.7, 130.8, 128.8, 128.4, 128.0 (2C), 127.9, 127.7, 124.4, 123.8, 121.4, 120.3, 118.9, 117.3; MALDI-MS (%): m/z=667 (100) $[M+H]^+$; HRMS found m/z: 667.2383 $[M+H]^+$; $C_{44}H_{27}N_8$ requires: 667.2359.

4.4. General procedure for the two-step in situ synthesis of spacer tunable bis-terpyridines (17–24)

To a 40 mL DMSO solution of terpyridine **8a** (or **8b**,**c**, 200 mg) was added bis(pinacolato)diboron **9** (1.1 equiv), KOAc (3.0 equiv), and $PdCl_2(PPh_3)_2$ (5 mol %). The solution was degassed and stirred at 80 °C under argon atmosphere for 6 h. The reaction vessel was recharged in situ with K_2CO_3 (3.0 equiv), dibromo coupling partner **16** (0.5 equiv), and $PdCl_2(PPh_3)_2$ (5 mol %). The mixture was then heated at 80–100 °C until the dibromo compound had disappeared as monitored by TLC. The catalyst was removed by filtration and washed thoroughly with $CHCl_3$ after the reaction mixture was cooled to room temperature. The filtrate was washed with H_2O (ca. 70 mL) for five times, and the organic layer was separated, dried over $MgSO_4$, then filtered, concentrated, and purified by column chromatography on activated basic Al_2O_3 (CH_2Cl_2/hexane=4:1–9:1, then pure CH_2Cl_2) to give the target compounds **17–24**.

*4.4.1. Spacer tunable bis-terpyridine **17***

White powder, 61% yield from **8a** and 1,3-dibromobenzene; ^{1}H NMR ($CDCl_3$) δ=8.82 (s, 4H), 8.75 (ddd, 4H, J_1=4.8 Hz, J_2=1.8 Hz, J_3=0.9 Hz), 8.69 (d, 4H, J=7.5 Hz), 8.05 (d, 4H, J=8.7 Hz), 7.98 (s, 1H), 7.89 (dt, 4H, J_1=7.5 Hz, J_2=1.8 Hz), 7.83 (d, 4H, J=8.7 Hz), 7.71 (dd, 2H, J_1=7.5 Hz, J_2=1.2 Hz), 7.60 (t, 1H, J=7.2 Hz), 7.37 (ddd, 4H, J_1=7.5 Hz, J_2=6.3 Hz, J_3=0.9 Hz); ^{13}C NMR ($CDCl_3$) δ=156.3, 156.0, 149.7, 149.1, 141.7, 141.1, 137.5, 136.8, 129.4, 127.8, 127.7, 126.5, 126.0, 123.8, 121.4, 118.7; MALDI-MS (%): m/z=693 (100) $[M+H]^+$; HRMS found m/z: 715.2563 $[M+Na]^+$; $C_{48}H_{32}N_6Na$ requires: 715.2563.

*4.4.2. Spacer tunable bis-terpyridine **18***

White powder, 59% yield from **8b** and 1,3-dibromobenzene; ^{1}H NMR ($CDCl_3$) δ=8.72 (s, 4H), 8.29 (d, 4H, J=7.5 Hz), 7.97 (d, 4H, J=8.1 Hz), 7.96 (s, 1H), 7.86 (d, 4H, J=8.1 Hz), 7.77 (t, 4H, J=8.1 Hz), 7.71 (dd, 2H, J_1=6.9 Hz, J_2=1.2 Hz), 7.62 (t, 1H, J=6.9 Hz), 6.83 (d, 4H, J=7.5 Hz), 4.11 (s, 12H); ^{13}C NMR ($CDCl_3$) δ=163.7, 156.0, 153.8, 149.5, 141.7, 141.3, 139.4, 138.5, 129.5, 127.9, 127.8, 126.5, 126.1, 118.6, 114.2, 111.1, 53.3; MALDI-MS (%): m/z=813 (100) $[M+H]^+$; HRMS found m/z: 813.3207 $[M+H]^+$; $C_{52}H_{41}N_6O_4$ requires: 813.3207.

*4.4.3. Spacer tunable bis-terpyridine **19***

White powder, 32% yield from **8c** and 1,3-dibromobenzene; ^{1}H NMR ($CDCl_3$) δ=8.90 (s, 4H), 8.88 (dd, 4H, J_1=8.4 Hz, J_2=1.2 Hz), 8.07–8.03 (m, 8H), 8.00 (s, 1H), 7.91 (dd, 4H, J_1=6.9 Hz, J_2=2.1 Hz), 7.78 (dd, 4H, J_1=7.8 Hz, J_2=1.2 Hz), 7.73 (dd, 2H, J_1=6.9 Hz, J_2=1.2 Hz), 7.65 (d, 1H, J=6.9 Hz); ^{13}C NMR ($CDCl_3$) δ=157.6, 154.3, 150.8, 142.5, 141.2, 137.9, 136.8, 133.6, 130.8, 129.6, 128.3, 128.1, 127.9, 126.7, 124.3, 120.3, 117.3; MALDI-MS (%): m/z=793 (100) $[M+H]^+$; HRMS found m/z: 815.2391 $[M+Na]^+$; $C_{52}H_{28}N_{10}Na$ requires: 815.2396.

*4.4.4. Spacer tunable bis-terpyridine **20***

White powder, 47% yield from **8a** and 2,6-dibromopyridine; ^{1}H NMR ($CDCl_3$) δ=8.83 (s, 4H), 8.76 (ddd, 4H, J_1=0.9 Hz, J_2=1.8 Hz, J_3=4.8 Hz), 8.69 (dt, 4H, J_1=0.9 Hz, J_2=8.1 Hz), 8.34 (d, 4H, J=8.4 Hz), 8.08 (d, 4H, J=8.4 Hz), 8.04 (d, 1H, J=8.7 Hz), 7.92–7.81 (m, 6H), 7.36 (ddd, 4H, J_1=0.9 Hz, J_1=4.8 Hz, J_3=7.5 Hz); ^{13}C NMR ($CDCl_3$) δ=156.5, 156.2, 149.9, 149.2, 140.1, 139.2, 137.6, 136.8, 127.9, 127.7, 127.6, 123.8, 121.4, 119.0, 118.9; MALDI-TOF MS: m/z 693.9 (100) $[M+H]^+$.

*4.4.5. Spacer tunable bis-terpyridine **21***

Pale yellow powder, 59% yield from **8a** and 2,5-dibromothiophene; ^{1}H NMR ($CDCl_3$) δ=8.79 (s, 4H), 8.75 (br d, 4H, J=4.8 Hz), 8.68 (d, 4H, J=7.8 Hz), 7.97 (d, 4H, J=8.4 Hz), 7.88 (ddd, 4H, J_1=0.9 Hz, J_2=1.8 Hz, J_3=7.8 Hz), 7.79 (d, 4H, J=8.4 Hz), 7.43 (s, 2H), 7.36 (ddd, 4H, J_1=0.9 Hz, J_2=4.8 Hz, J_3=7.5 Hz); ^{13}C NMR ($CDCl_3$) δ=156.3, 156.1, 149.5, 149.2, 143.5, 137.6, 136.9, 135.0, 127.9, 126.1, 124.7, 123.8, 121.4, 118.6; MALDI-TOF MS: m/z 698.1 (100) $[M]^+$.

*4.4.6. Spacer tunable bis-terpyridine **22***

Pale yellow powder, 48% yield from **8a** and 2,5-dibromo-3-octylthiophene; ^{1}H NMR ($CDCl_3$) δ=8.82–8.75 (m, 8H), 8.69 (d, 4H, J=7.8 Hz), 8.06–7.76 (m, 11H), 7.65 (d, 2H, J=8.1 Hz), 7.36 (br t, 4H, J=6.3 Hz), 2.75 (t, 2H, J=7.5 Hz), 1.72 (m, 2H), 1.28 (m, 10H), 0.88 (t, 3H, J=6.6 Hz); ^{13}C NMR ($CDCl_3$) δ=156.3 (2C), 156.0, 149.7 (2C), 149.2, 141.8, 141.0, 140.5, 137.7, 137.3 (2C), 136.9, 135.4, 135.1, 129.6, 127.8, 127.6, 127.5, 126.4, 125.9, 123.8, 121.4, 118.7 (2C), 118.5, 31.9, 31.1, 29.7, 29.4, 29.3, 29.1, 22.6, 14.1; MALDI-TOF MS: m/z 833.5 (100) $[M+Na]^+$.

Acknowledgements

We thank the Ministry of Education, Culture, Sports, Sciences, and Technology, Japan for financial support.

References and notes

1. For recent reviews, see: (a) Cooke, M. W.; Hanan, G. S. *Chem. Soc. Rev.* **2007**, *36*, 1466; (b) Constable, E. C. *Chem. Soc. Rev.* **2007**, *36*, 246; (c) Kurth, D. G.; Higuchi, M. *Soft Matter* **2006**, *2*, 915; (d) Medlycott, E. A.; Hanan, G. S. *Chem. Soc. Rev.* **2005**, *34*, 133; (e) Andres, P. R.; Schubert, U. S. *Adv. Mater.* **2004**, *16*, 1043.
2. Mortimer, R. J.; Dyer, A. L.; Reynolds, J. R. *Displays* **2006**, *27*, 2 and references therein.
3. For recent research articles, see: (a) Cooke, M. W.; Hanan, G. S.; Loiseau, F.; Campagna, S.; Watanabe, M.; Tanaka, Y. *J. Am. Chem. Soc.* **2007**, *129*, 10479; (b) Camerel, F.; Ziessel, R.; Donnio, B.; Bourgogne, C.; Guillon, D.; Schmutz, M.; Iacovita, C.; Bucher, J. P. *Angew. Chem., Int. Ed.* **2007**, *46*, 2659; (c) Song, B.;

Wang, G.; Tan, M.; Yuan, J. *J. Am. Chem. Soc.* **2006**, *128*, 13442; (d) Carlson, C. N.; Kuehl, C. J.; Da-Re, R. E.; Veauthier, J. M.; Schelter, E. J.; Milligan, A. E.; Scott, B. L.; Bauer, E. D.; Thompson, J. D.; Morris, D. E.; John, K. D. *J. Am. Chem. Soc.* **2006**, *128*, 7230; (e) Lainé, P. P.; Bedioui, F.; Loiseau, F.; Chiorboli, C.; Campagna, S. *J. Am. Chem. Soc.* **2006**, *128*, 7510; (f) Sénéchal-David, K.; Leonard, J. P.; Plush, S. E.; Gunnlaugsson, T. *Org. Lett.* **2006**, *8*, 2727; (g) Coppo, P.; Duati, M.; Kozhevnikov, V. N.; Hofstraat, J. W.; De Cola, L. *Angew. Chem., Int. Ed.* **2005**, *44*, 1806.

4. (a) Cheon, J.-D.; Mutai, T.; Araki, K. *Org. Biomol. Chem.* **2007**, *5*, 2762; (b) Yuan, S.-C.; Chen, H.-B.; Zhang, Y.; Pei, J. *Org. Lett.* **2006**, *8*, 5701; (c) Goodall, W.; Wild, K.; Arm, K. J.; Williams, J. A. G. *J. Chem. Soc., Perkin Trans. 2* **2002**, 1669; (d) Loren, J. C.; Siegel, J. S. *Angew. Chem., Int. Ed.* **2001**, *40*, 754; (e) Mutai, T.; Cheon, J.-D.; Arita, S.; Araki, K. *J. Chem. Soc., Perkin Trans. 2* **2001**, 1045.
5. (a) Auffrant, A.; Barbieri, A.; Barigelletti, F.; Collin, J. P.; Flamigni, L.; Sabatini, C.; Sauvage, J. P. *Inorg. Chem.* **2006**, *45*, 10990; (b) Yu, S.-C.; Kwok, C.-C.; Chan, W.-K.; Che, C.-M. *Adv. Mater.* **2003**, *15*, 1643.
6. (a) Constable, E. C.; Housecroft, C. E.; Smith, C. B. *Inorg. Chem. Commun.* **2003**, *6*, 1011; (b) Newkome, G. R.; Cho, T. J.; Moorefield, C. N.; Cush, R.; Russo, P. S.; Godínez, L. A.; Saunders, M. J.; Mohapatra, P. *Chem.—Eur. J.* **2002**, *8*, 2946.
7. (a) Han, F. S.; Higuchi, M.; Kurth, D. G. *J. Am. Chem. Soc.* **2008**, *130*, 2073; (b) Han, F. S.; Higuchi, M.; Kurth, D. G. *Adv. Mater.* **2007**, *19*, 3928; (c) Harriman, A.; Mayeux, A.; Nicola, A. D.; Ziessel, R. *Phys. Chem. Chem. Phys.* **2002**, *4*, 2229.
8. Sauvage, J. P.; Collin, J. P.; Chambron, J. C.; Guillerez, S.; Coudret, C.; Balzani, V.; Barigelletti, F.; Cola, L. D.; Flamigni, L. *Chem. Rev.* **1994**, *94*, 993 and references therein.
9. Eryazici, I.; Moorefield, C. N.; Durmus, S.; Newkome, G. R. *J. Org. Chem.* **2006**, *71*, 1009 and references therein.
10. (a) Andres, P. R.; Lohmeijer, B. G. G.; Hofmeier, H.; Schubert, U. S. *Synthesis* **2003**, 2865; (b) Newkome, G. R.; He, E. *J. Mater. Chem.* **1997**, *7*, 1237.
11. Han, F. S.; Higuchi, M.; Kurth, D. G. *Org. Lett.* **2007**, *9*, 559 and references therein.
12. Okamura, R.; Wada, T.; Aikawa, K.; Nagata, T.; Tanaka, K. *Inorg. Chem.* **2004**, *43*, 7210.
13. (a) Ishiyama, T.; Itoh, Y.; Kitano, T.; Miyaura, N. *Tetrahedron Lett.* **1997**, *38*, 3447; (b) Ishiyama, T.; Murata, M.; Miyaura, N. *J. Org. Chem.* **1995**, *60*, 7508.
14. Miyaura, N.; Suzuki, A. *Chem. Rev.* **1995**, *95*, 2457 and references therein.
15. (a) Sauvage, J. P.; Ward, M. *Inorg. Chem.* **1991**, *30*, 3869; (b) Thompson, A. M. W. C. *Coord. Chem. Rev.* **1997**, *160*, 1.
16. The assignment of NMR peaks of compounds **12**, **23**, and **24** are difficult due to the weak signals caused by their somewhat poor solubility. However, mass spectrometry revealed characteristic peaks of m/z=717.21 (M^+), 779.9 (M^+), and 900.6 (M^+) corresponding to **12**, **23**, and **24**, respectively.
17. Fang, Y.; Taylor, N. J.; Laverdière, F.; Hanan, G. S.; Loiseau, F.; Nastasi, F.; Campagna, S.; Nierengarten, H.; Leize-Wagner, E.; Dorsselaer, A. V. *Inorg. Chem.* **2007**, *46*, 2854.
18. The quantum yields (Φ_f) were evaluated according to the method described in the literature using compound **5** in dichloromethane (Φ_f=0.13, see Ref. 5a) as standard, see: Brooks, J.; Babayan, Y.; Lamansky, S.; Djurovich, P. I.; Tsyba, I.; Bau, R.; Thompson, M. E. *Inorg. Chem.* **2002**, *41*, 3055.
19. The Lippert's function Δf is used to evaluate the solvent polarity without considering the protic nature of MeOH. The Δf of cyclohexane, CH_2Cl_2, CH_3CN, and MeOH are 0.00, 0.21, 0.305, and 0.309, respectively. These parameters are taken from Ref. 4d and following reference: Ababneh, A. M.; Large, C. C.; Georghiou, S. *J. Appl. Sci. Res.* **2007**, *3*, 1288.
20. Wasielewski, M. R.; Minsek, D. W.; Niemczyk, M. P.; Svec, W. A.; Yang, N. C.-C. *J. Am. Chem. Soc.* **1990**, *112*, 2823.
21. Harriman, A.; Hissler, M.; Ziessel, R. *Phys. Chem. Chem. Phys.* **1999**, *1*, 4203.